

# Improved position-signal-difference electric near-field measurements based on fringe capacitance model

Hiroki Funato<sup>1a)</sup>, Takashi Suga<sup>1</sup>, and Michihiko Suhara<sup>2</sup>

<sup>1</sup> Yokohama Research Laboratory, Hitachi, Ltd.,

292 Yoshida-cho, Totsuka-ku, Yokohama, Kanagawa 244–0813, Japan

<sup>2</sup> Department of Electrical and Electronic Engineering, Graduate School of Science and Engineering, Tokyo Metropolitan University,

1–1 Minami-Osawa, Hachioji, Tokyo 192–0397, Japan

a) [hiroki.funato.ss@hitachi.com](mailto:hiroki.funato.ss@hitachi.com)

**Abstract:** An approach based on the analytical expressions of the fringe capacitance for describing the spatial resolution for Position Signal Difference (PSD) electric near-field measurements is addressed in this paper. The calculated full width at half maximum (FWHM) of the measured results by using PSD for the scanning over microstrip line using the proposed model were in good agreement with the measurement results. Furthermore, a new measurement technique for obtaining more accurate results of a normal component of electric near-field by eliminating the fringe capacitance is proposed. The demonstrated results when using the proposed method showed a better correlation to the simulated normal component of electric field than using conventional PSD. Finally, the role of probe displacement for Double Position Signal Difference (DPSD) measurements is also clarified by verifying the measurements using the electromagnetic simulated results.

**Keywords:** electric near-field, Position Signal Difference (PSD)

**Classification:** Microwave and millimeter wave devices, circuits, and systems

## References

- [1] Y. Gao and I. Wolff: IEEE Trans. Microwave Theory Tech. **46** (1998) 907. DOI:10.1109/22.701442
- [2] D. Baudry, C. Arcambal, A. Louis, B. Mazari and P. Eudeline: IEEE Trans. Electromagn. Compat. **49** (2007) 485. DOI:10.1109/TEMC.2007.902194
- [3] D. Uchida, T. Nagai, Y. Oshima and S. Wakana: IEEE Radio and Wireless Symposium (RWS) (2011) 299. DOI:10.1109/RWS.2011.5725457
- [4] R. Kantor and I. V. Shvets: IEEE Trans. Microwave Theory Tech. **51** (2003) 2228. DOI:10.1109/TMTT.2003.818938
- [5] H. Funato, T. Suga and M. Suhara: IEEE Int. Electromagn. Compat. Symp. (2013) 621. DOI:10.1109/ISEMC.2013.6670486
- [6] A. Bansal, B. C. Paul and K. Roy: IEEE Trans. Electron. Dev. **52** (2005) 256. DOI:10.1109/TED.2004.842713

## 1 Introduction

Electric near-field measurements are one of the essential techniques for revealing the RF behavior of electronics by visualizing the field distributions, especially in the area of electromagnetic compatibility [1, 2]. The spatial resolution for such near-field measurements is one of key performance parameters. A number of works on miniaturized probes have been reported so far in order to create a finer resolution [3]. As an alternative way, PSD and DPSD are helpful methods for obtaining finer or required spatial resolutions without needing to fabricate a miniaturized probe [4, 5]. However, no work has been conducted to clarify the quantitative description of the spatial resolution with respect to the PSD method. Moreover, the contribution of the probe displacement, which is a key parameter for both PSD and DPSD, to the results has yet to be clarified.

An approach to describing the spatial resolution of the PSD measurement results is presented in this paper. Furthermore, the improved measurement technique to eliminate the fringe capacitance when attempting to obtain more accurate normal components of electric field is then proposed. The role of the probe displacement for DPSD is also clarified by comparing the measurement results with electromagnetic simulated results. All these clarifications contribute to making the near-field measurements using the PSD/DPSD methods more efficient and useful.

## 2 Fringe capacitance model

The probe and measurement setup used for the modeling and validations are shown in Fig. 1. A three-layered printed circuit board is used for the monopole electric near-field probe. The surface layers have a 2-mm-wide ground and the inner layer has a signal element tip, which is 0.28-mm wide, 1-mm long and 18- $\mu\text{m}$  thick. The conductors are made of copper and the substrate is FR-4 with 0.3-mm between the layers. The probe is connected to port 2 of network analyzer 8753D and the microstrip line (MSL) with a 50-ohm termination is connected to port 1 during the measurements. The frequency response of  $S_{21}$  is then observed at 1 GHz with scanning the probe along the  $x$ -axis, as shown in Fig. 1, at 0.1-mm steps. The measurements were performed at various probe heights to obtain the PSD-processed result  $I_{PSD}$  based on the following definition of PSD [4].

$$I_{PSD} = I_1 - I_2 \quad (1)$$

where the measured value is expressed as electric current based on the consideration that the current is induced due to the electric near-field [1]. The probe height  $h_p$  for  $I_1$  in the measurements is fixed to 0 mm, and the height for  $I_2$  is set to  $h_p + d_p$ , where the displacement  $d_p$  is varied from 0.1 to 0.7 mm.

Fig. 2 shows an example of the PSD-processed results for different probe displacements  $d_p$ . It can be seen that the full width at half maximum (FWHM)  $w_{fw}$ , which is generally used to evaluate the spatial resolution of

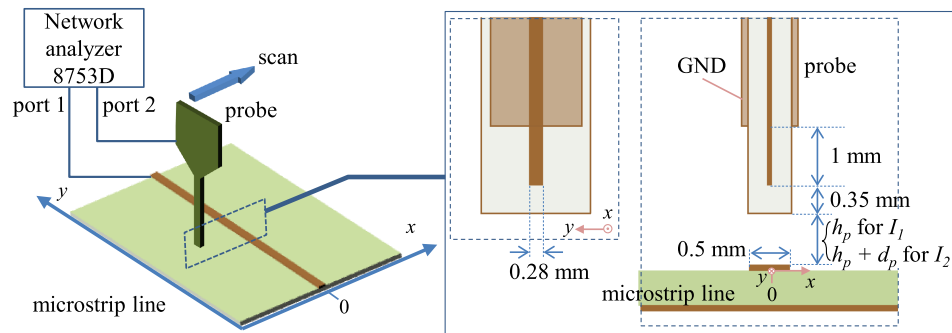


**Fig. 1.** Probe and setup for PSD/DPSD measurements

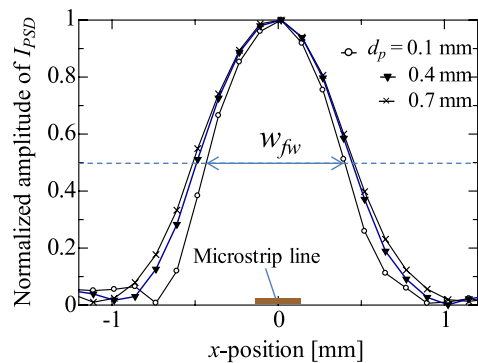


**Fig. 2.** PSD measurement results with changing shift parameter  $d_p$  at 1 GHz

the measurements, is varied depending on the  $d_p$ . Since the  $d_p$  is the key parameter for PSD, it is very important to understand this aspect.

We assume the amplitude of the signal detected by the probe can be described by focusing on several of the fringe capacitances, as shown in Fig. 3. The figure shows the definitions of the capacitance between each portion of the probe tip and the trace, where  $C_s$  is the capacitance between the side of probe and the surface of the trace and  $C_b$  is between the bottom of the probe and the side of the trace. These fringe capacitances are calculated using the following equations [6].

$$C_n(L_e, W_m) = \frac{2\varepsilon W_p}{\pi} \ln \left( \frac{s + \eta W_m + \sqrt{h^2 + (\eta W_m)^2 + 2s\eta W_m}}{s + h} \right) \quad (2)$$

$$\eta = \exp\left(\frac{L_e + h - \sqrt{h^2 + W_m^2 + 2sW_m}}{3.7L_e}\right) \quad (3)$$

where  $W_p$  is the width of the probe tip (0.28 mm),  $\varepsilon$  is the permeability,  $s$  is the separation of the probe from the trace edge, and  $h$  is the probe height.  $L_e$  is the length of the probe tip element (1 mm) for the calculation of  $C_s$  and the thickness of MSL (50  $\mu\text{m}$ ) for  $C_b$ ,  $W_m$  is the trace width of MSL (0.5 mm) for  $C_s$  and the thickness of the probe element (18  $\mu\text{m}$ ) for  $C_b$ . Therefore,  $C_s$  and  $C_b$  can be calculated as

$$C_s = C_n(1 \text{ mm}, 0.5 \text{ mm}) \quad (4)$$

$$C_b = C_n(50 \mu\text{m}, 18 \mu\text{m}) \quad (5)$$

$C_f$  is the capacitance between the corners of the probe tip and the trace, which can be expressed as follows [6].

$$C_f = \frac{0.1\epsilon W_p}{\pi} \ln\left(\frac{\pi W_p}{\sqrt{h^2 + s^2}}\right) e^{\left|-\frac{h-s}{h+s}\right|} \quad (6)$$

Fig. 4 indicates the calculated FWHM using the fringe capacitance model above while comparing it to the measurement results with different  $d_p$ . The difference between the calculated and measured results is within 13%, which is a good correlation. The notable aspect is that selecting a greater  $d_p$  value makes the spatial resolution worse for PSD due to the increase in fringe capacitance between the probe element and the trace. It is clear from the equations above that this fringe capacitance depends on not only the shape of the probe tip but also the dimensions of the targeting trace. Therefore, it is important to select an appropriate  $d_p$  in order to obtain the required spatial resolution with respect to the finest trace in the device under testing, which can be derived using the model addressed.

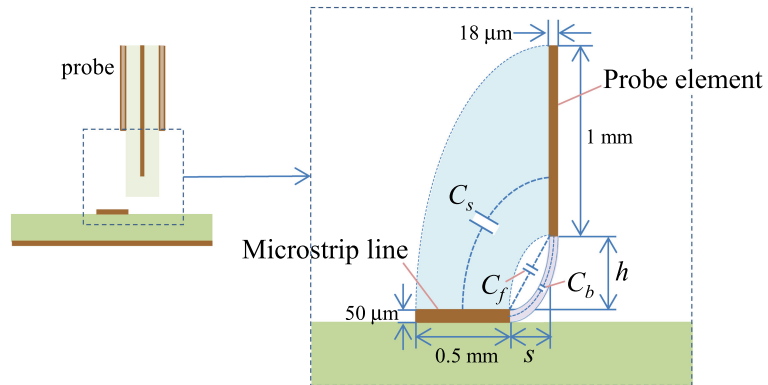


**Fig. 3.** Fringe capacitance model between probe element and trace

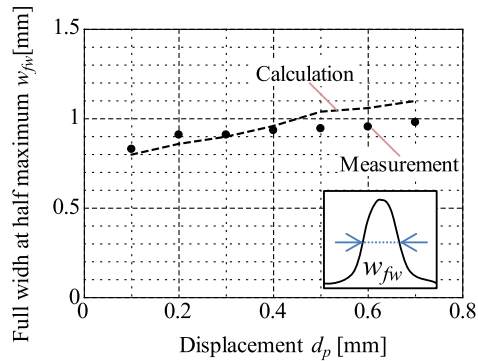


**Fig. 4.** Calculated FWHM  $w_{fw}$  compared to measurements with various  $d_p$

### 3 Improved PSD method

It was revealed that the fringe capacitance between the probe element and target is the factor that causes the degradation of the spatial resolution discussed in the previous section. Since the fringe capacitance to the side of the probe is considered to correspond to the tangential component of the electric near-field, it is important to use a smaller  $d_p$  displacement value for the measurement of the normal component of an electric field. However, the limit of the finer displacement is normally decided due to the performance of the manipulation hardware and its repeatability/stability, e.g., the probe manipulator used for this study can handle a displacement value  $d_p$  down to 100  $\mu\text{m}$  in order to maintain good repeatability. Therefore, it is required to eliminate the fringe capacitance without needing the finer displacements of probe. The new measurement technique for eliminating the fringe capacitance is proposed in this section. Fig. 5 shows the procedure for taking the measurements. It requires two sets of PSD results obtained by using the same displacement  $d_p$ , which are defined as  $I_{PSD1}$  and  $I_{PSD2}$ . When taking into account that the remaining fringe capacitance  $C_a$  is nearly equal to  $C_b$ , only the capacitances related to the normal component remain by subtracting  $I_{PSD2}$  from  $I_{PSD1}$ , as can be determined using the following equation.

$$\begin{aligned} I_{PSD1} - I_{PSD2} &= (I_1 - I_2) - (I_2 - I_3) = I_1 - 2I_2 + I_3 \\ &= C_{z1} - C_{z2} + 2C_a - 2C_b \simeq C_{z1} - C_{z2} \end{aligned} \quad (7)$$

where  $I_1$ ,  $I_2$ , and  $I_3$  are the measured results at different probe heights. The fringe capacitance to the corner of the probe tip is neglected since it is sufficiently small. As in the equation, this method can be processed using the three sets of results  $I_1$ ,  $I_2$ , and  $I_3$  acquired using the same displacements  $d_p$ . The processed result when using the proposed method is shown in Fig. 6(b) with the comparison to conventional PSD and the normal component of electric field  $E_z$  obtained by electromagnetic simulation at  $z = 0.35 \text{ mm}$  as defined in Fig. 6(a), where  $d_p$  was set to 0.1 mm for  $I_{PSD1}$  and  $I_{PSD2}$  and the separation of the probe tip from the trace was 0.35 mm. It is obvious that the proposed method shows better matching with the simulated  $E_z$  than the conventional PSD without using the finer displacements of probe. The only disadvantage of using this method is that the signal level is also reduced by the repeated subtractions, but this would not become a serious problem since the field of interest is normally strong for EMC applications.

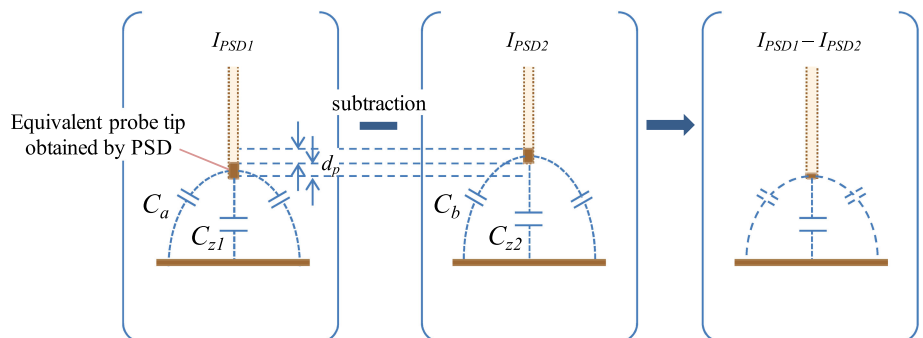
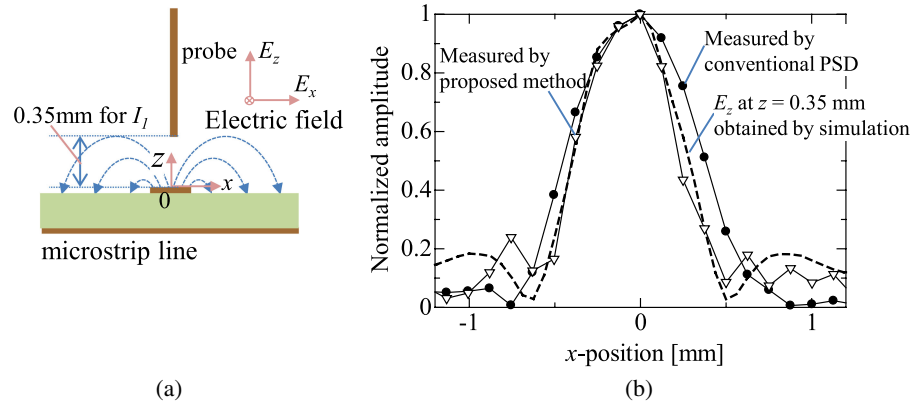


Fig. 5. Procedure of proposed method



**Fig. 6.** (a) Definitions of parameters and (b) Comparison between conventional PSD and proposed method

#### 4 Role of probe displacement ( $d_p$ ) for DPSD

Since the probe displacement  $d_p$  is a common parameter for PSD and DPSD, it is very important to understand its meaning and effect not only for PSD but also for DPSD. The DPSD measurement results can be obtained by using the process in the following equation along with the same definitions as in Eq. (1) [5].

$$I_{DPSD} = I_2 - I_{PSD} = I_2 - (I_1 - I_2) = 2I_2 - I_1 \quad (8)$$

DPSD is also the post process for eliminating the normal component of the electric near-field coupling between the probe tip and targeting trace, and the fringe capacitance remains. Therefore, we believe changing the probe displacement  $d_p$  is equivalent to changing the measurement height of the tangential electric field. This assumption is verified by comparing the DPSD processed results at different  $d_p$  to the tangential component of electric field  $E_x$  obtained from an electromagnetic simulation at the corresponding heights. The results are shown in Fig. 7, where the definition of the parameter is as shown in Fig. 8(a). In order to compare these results, the peak-to-peak distances  $d_t$  as shown in the inset of Fig. 8(b) were evaluated as one feature parameter and summarized in Fig. 8(b). From this comparison, the change in probe displacement

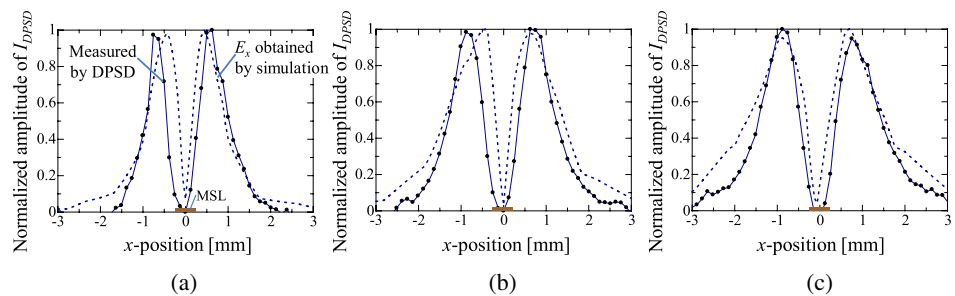


**Fig. 7.** DPSD measurement results at different  $d_p$  comparing to  $E_x$  obtained by electromagnetic simulation. (a)  $d_p = 0.1$  mm,  $E_x$  at  $z = 0.45$  mm (b)  $d_p = 0.4$  mm,  $E_x$  at  $z = 0.75$  mm (c)  $d_p = 0.7$  mm,  $E_x$  at  $z = 1.05$  mm

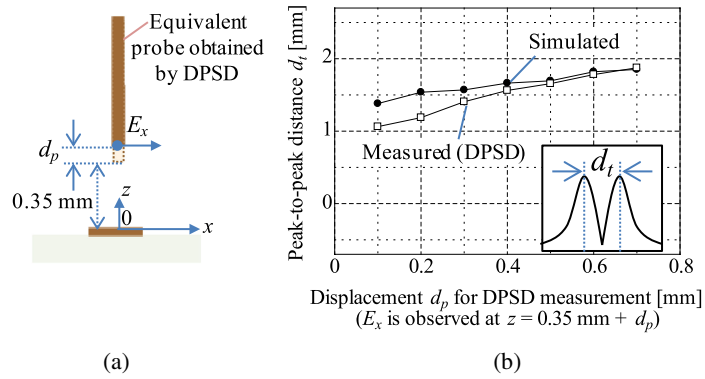


**Fig. 8.** (a) Configuration for measurements and simulation  
(b) Comparison of peak-to-peak distance  $d_t$  between measurements at various  $d_p$  and simulation results

ment  $d_p$  provides a good correlation to the change in observation height for a tangential electric field  $E_x$ .

## 5 Conclusion

An approach to quantitatively calculate the full width at half maximum by using the fringe capacitances for PSD electric near-field measurements is addressed and verified. Such spatial resolutions were revealed to be affected by the probe displacement in PSD and a greater  $d_p$  value makes the resolution worse. A new measurement method was proposed based on this fact in order to improve the measurement accuracy of the normal component of an electric field without needing finer manipulation of the probe by eliminating the fringe capacitance to the side of it. The proposed method showed a better level of matching to the simulated results than conventional PSD. The meaning and the probe displacement parameter effect for DPSD also have been clarified by comparing them to the simulated results. These clarifications and proposed enhanced method allow PSD and DPSD to be more effective and practical in near-field measurements.